Inorganic Chemistry

ARTICLE

pubs.acs.org/IC

Vanadium-Based Pro-Catalysts Bearing Depleted 1,3-Calix[4]arenes for Ethylene or ε-Caprolactone Polymerization

Lucy Clowes, Carl Redshaw,* and David L. Hughes

Energy Materials Laboratory, School of Chemistry, University of East Anglia, Norwich NR4 7TJ, U.K.

Supporting Information

ABSTRACT: Reaction of [V(X)(OR)$_3$] (X = O, N*p*-tolyl, R = *n*Pr, *t*Bu) with 5,11,17,23-*t*Bu-25,27-dihydroxycalix[4]arene (LH$_2$) led to the formation of [V(X)(OR)L]$_2$ X = O, R = *n*Pr (**1**); X = N*p*-tolyl, R = *n*Pr (**2**); X = N*p*-tolyl, R = *t*Bu (**3**) as the major product. In the case of X = O, the minor hydrolysis product {[VO(O*n*Pr)]$_2$(μ-O)L}$_2$ (**4**) has also been characterized. Complexes (**1**)−(**4**), in the presence of the co-catalyst dimethylaluminum chloride and the reactivator ethyltrichloroacetate, are highly active (≤16,400 g/mmol h bar), thermally stable pro-catalysts for the polymerization of ethylene. The use of silica supports with (**1**) and (**2**) under slurry conditions yielded polymer with activities ≤30 g/mmol h. Complexes (**1**)−(**3**) have also been screened as pro-catalysts for the ring-opening polymerization of ε-caprolactone; the conversion rate order (**1**) (94%) > (**2**) (46%) > (**3**) (20%) was observed at 80 °C over 72 h.

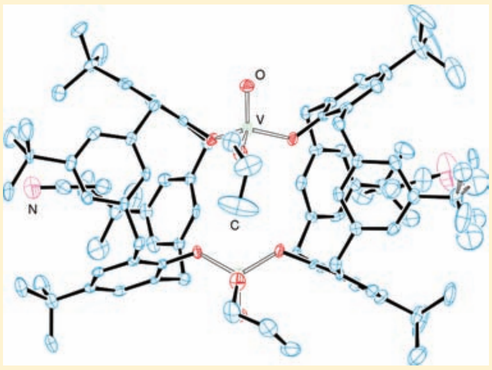

1. INTRODUCTION

Calixarenes are emerging as a versatile family of ancillary ligands in a variety of catalytic processes.[1] In the area of α-olefin polymerization catalysis, notably high catalytic activities have been achieved for vanadium-based pro-catalysts bearing calixarenes, particularly when the calixarene bears a dimethyleneoxa ($-CH_2OCH_2-$) linkage.[2] Similarly, high activities have also been achieved with bi- and linear triphenols bearing methylene ($-CH_2-$) bridges.[3] Depleted calixarenes can be viewed as cyclic analogues of such biphenols, and synthetic routes to 1,2- and 1,3-depleted calix[4]arenes are now available.[4] However, the coordination chemistry of such depleted calixarenes is only just emerging,[5] and their use in olefin polymerization catalysis is restricted to a patent on group IV systems,[6] and more recently a number of titanacalix[4]arenes, and tantacalix[4]arenes.[7] Herein, we report the synthesis, characterization, and ethylene polymerization behavior of the complexes [VO(O*n*Pr)L]$_2$ (**1**), [V(N*p*-tolyl)(O*n*Pr)L]$_2$ (**2**), [V(N*p*-tolyl)(O*t*Bu)L]$_2$ (**3**), and {[VO(O*n*Pr)]$_2$(μ-O)L}$_2$ (**4**), bearing ligands derived from the 1,3-depleted ligand 5,11,17,23-*t*Bu-25,27-dihydroxycalix[4]arene (LH$_2$), see Chart 1.

2. EXPERIMENTAL SECTION

2.1. General Information. All manipulations, unless otherwise stated, were carried out under an atmosphere of dry nitrogen using conventional Schlenk and cannula techniques or in a conventional nitrogen-filled glovebox. Toluene was refluxed over sodium, and acetonitrile over calcium hydride. All solvents were distilled and degassed prior to use. Dry methanol or ethanol was stored over activated 4 Å molecular sieves. ε-Caprolactone was dried over calcium hydride, vacuum distilled and degassed prior to use. IR spectra (nujol mulls, KBr windows) were recorded on a Nicolet Avatar 360 FT IR spectrometer. ^{51}V, ^{13}C, and ^{1}H NMR spectra were recorded at room temperature on a Varian VXR 400 S spectrometer at 400 MHz and a Gemini 300 NMR spectrometer or a Bruker Avance DPX-300 spectrometer at 300 MHz. The ^{1}H NMR spectra were calibrated against the residual protio impurity of the deuterated solvent. Elemental analyses were performed by the elemental analysis service at the London Metropolitan University. [V(N*p*-tolyl)(OR)$_3$] (R = *n*Pr or *t*Bu) were made using the method of Lutz et al.[8]

2.2. Synthesis of the Vanadium Complexes. *2.2.0. General Procedure.* Excess (2.2 equiv) of [VO(O*n*Pr)$_3$] or [V(N*p*-tolyl)(OR)$_3$] (R = *n*Pr, *t*Bu) was added to a solution of ligand in 30 mL of toluene. The reaction mixture was stirred at reflux for 12 h. The reaction solution was cooled to room temperature, and volatiles were removed under vacuo. The solid residue was extracted into hot acetonitrile. After prolonged standing at room temperature the product was formed.

*2.2.1. Synthesis of [VO(OnPr)L]$_2$ (**1**).* Obtained as dark red plates in 0.47 g, 39% yield. Elemental analysis calcd (%) for $V_2C_{94}H_{122}O_8$: C 76.18, H 8.30; found C 76.03, H 8.21. MS (E.S.): *m*/*z*: 1379 [M − O-2^{n}Pr]$^+$, 1297 [M$^+$ − VO]$^+$, 1280 [M$^+$ − O2H]$^+$. IR (cm^{-1}) ν(V═O) 978. ^{1}H NMR (CDCl$_3$): δ = 7.11 (s, 1H, Ar*H*), 7.06 (s, 3H, Ar*H*), 6.95 (s, 9H, Ar-*H*), 6.93 (s, 4H, Ar*H*), 5.01−4.9 (m, 4H, OC*H*$_2$CH$_2$CH$_3$), 4.60 (dd, 8H, J_1 =5.50, J_2 = 13.71, ArC*H*$_2$Ar), 3.60 (d, 4H, J = 14.12, ArC*H*$_2$Ar), 3.30 (d, 4H, J = 13.68, ArC*H*$_2$Ar), 1.90 (s, 3H, C*H*$_3$CN), 1.70 (m, 4H, OCH$_2$C*H*$_2$CH$_3$), 1.32 (s, 36H, C(C*H*$_3$)$_3$), 1.22 (s, 18H, C(C*H*$_3$)$_3$), 1.10 (s, 18H, C(C*H*$_3$)$_3$), 0.80 (t, 6H, J = 7.38, OCH$_2$CH$_2$C*H*$_3$). Selected ^{13}C NMR (C$_6$D$_6$): δ = 88.1 (CH$_2$), 33.5, 31.7 (C(CH$_3$)$_3$). ^{51}V NMR (CDCl$_3$): δ = −533.32 ($\omega_{1/2}$ 140 Hz).

*2.2.2. Synthesis of [V(Np-tolyl)(OnPr)L]$_2$ (**2**).* Obtained as yellow plates in 0.57 g, 43% yield. Elemental analysis calcd (%) for

Received: May 14, 2011
Published: July 12, 2011

Chart 1. Pro-Catalysts (1)−(4)

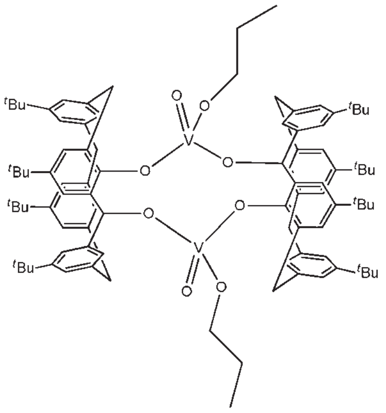

(1)

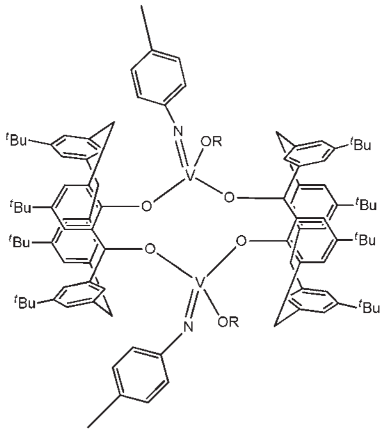

(2) R = O^{n}Pr, **(3)** R = O^{t}Bu

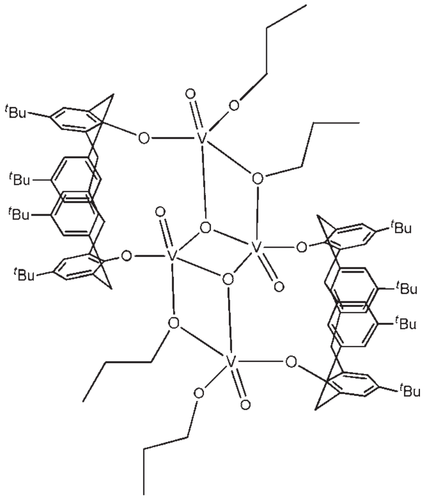

(4)

$V_2C_{108}H_{136}N_2O_6$: C 78.14, H 8.26, N 1.69; found C 77.93, H 8.13, N 1.78. MS (E.S.): *m/z*: 1660 [M]$^+$, 1600 [M$^+$ − O*n*Pr]. IR (cm^{-1}) ν(V═N) 1098. ^{1}H NMR (CDCl$_3$): δ = 7.79 (s, 2H, Ar*H*), 7.71 (s, 1H, Ar*H*), 7.10−7.05 (overlapping m, 10H, Ar*H*), 6.90 (d, 4H, Ar*H*), 6.74 (s, 4H, Ar*H*), 6.70 (d, 3H, *J* = 8.23, Ar*H*), 6.10 (d, 4H, *J* = 8.19, Ar*H*), 5.00 (m, 4H, OC*H*$_2$CH$_2$CH$_3$), 4.76 (dd, 8H, J_1 = 13.11, J_2 = 22.47, ArC*H*$_2$Ar), 3.50 (d, 4H, *J* = 12.23, ArC*H*$_2$Ar), 3.10 (d, 4H, *J* = 12.96, ArC*H*$_2$Ar), 2.22 (s, 6H, NptolC*H*$_3$), 1.96 (s, 3H, C*H*$_3$CN), 1.85 (m, 4H, OCH$_2$C*H*$_2$CH$_3$), 1.27 (s, 18H, C(C*H*$_3$)$_3$), 1.19 (s, 36H, C(C*H*$_3$)$_3$), 1.16 (s, 18H, C(C*H*$_3$)$_3$), 0.80 (t, 6H, *J* = 7.43, OCH$_2$CH$_2$C*H*$_3$). Selected ^{13}C NMR (C$_6$D$_6$): δ = 83.2 (CH$_2$), 32.9, 30.3 (C(CH$_3$)$_3$). ^{51}V NMR (CDCl$_3$): δ = −486.89 ($\omega_{1/2}$ 335 Hz).

*2.2.1. Synthesis of [V(Np-tolyl)(OtBu)L]$_2$ (**3**).* Obtained as yellow/orange plates in 0.53 g, 40% yield. Elemental analysis calcd (%) for $V_2C_{110}H_{140}N_2O_6$: C 78.26, H 8.36, N 1.66; found C 78.17, H 8.26, N 1.76. MS (E.S.): *m/z*: 1688 [M]$^+$, 1632 [M − *t*Bu]$^+$,1558 [M − O*t*Bu]$^+$. IR (cm^{-1}) ν(V═N) 1093. ^{1}H NMR (CDCl$_3$): δ = 7.65 (s, 1H, Ar*H*), 7.56 (s, 1H, Ar*H*), 7.15 (s, 2H, Ar*H*), 7.05−6.82 (overlapping m, 10H, Ar*H*), 6.68 (s, 4H, Ar*H*), 6.52 (d, 4H, *J* = 8.08, Ar*H*), 6.40 (d, 6H, *J* = 8.25, Ar*H*), 4.70 (d, 4H, *J* = 15.27, ArC*H*$_2$Ar), 4.55 (d, 4H, *J* = 14.12, ArC*H*$_2$Ar), 3.70 (overlapping m, 8H, ArC*H*$_2$Ar), 2.38 (s, 6H, NptolC*H*$_3$), 2.00 (s, 3H, C*H*$_3$CN), 1.58−1.44 (overlapping m, 81H, C(C*H*$_3$)$_3$), 1.33 (s, 9H, C(C*H*$_3$)$_3$). Selected ^{13}C NMR (C$_6$D$_6$): δ = 82.8 (CH$_2$), 31.7, 30.5 (C(CH$_3$)$_3$). ^{51}V NMR (CDCl$_3$): δ = −602.19 ($\omega_{1/2}$ 400 Hz), −608.08 ($\omega_{1/2}$ 400 Hz).

*2.2.4. Synthesis of {[VO(OnPr)]$_2$(μ-O)L}$_2$ (**4**).* Obtained as dark red clusters in 0.39 g, 27% yield. Elemental analysis calcd (%) for $V_4C_{100}H_{136}O_{14}$: C 68.01, H 7.76; found C 68.12, H 7.60. MS (E.S.): *m/z*: 1765 [M]$^+$, 1722 [M$^+$ − *n*Pr]$^+$. IR (cm^{-1}) ν(V═O) 974. ^{1}H NMR (CDCl$_3$): δ =7.25−7.22 (m, 1H, Ar*H*), 7.17−7.10 (m, 8H, Ar*H*), 7.0−6.90 (m, 8H, Ar-*H*), 6.19 (s, 2H, Ar*H*), 6.05(s, 1H, Ar*H*), 5.47−5.14 (overlapping m, 8H, OC*H*$_2$CH$_2$CH$_3$), 4.78 (dd, 4H, J_1 =15.85, J_2 = 22.33, ArC*H*$_2$Ar), 4.10 (dd, 4H, J_1 = 15.61, J_2 = 25.54, ArC*H*$_2$Ar), 3.75 (t, 4H, *J* = 14.58, ArC*H*$_2$Ar), 3.60 (d, 4H, *J* = 14.76, ArC*H*$_2$Ar), 1.95 (s, 3H, C*H*$_3$CN), 1.80 (m, 8H, OCH$_2$C*H*$_2$CH$_3$), 1.32 (s, 25H, C(C*H*$_3$)$_3$), 1.22 (s, 46H, C(C*H*$_3$)$_3$), 1.00 (t, 12H, *J* = 7.37, OCH$_2$CH$_2$C*H*$_3$). Selected ^{13}C NMR (C$_6$D$_6$): δ = 90.6, 78.8 (CH$_2$), 36.6, 31.4 (C(CH$_3$)$_3$). ^{51}V NMR (CDCl$_3$): δ = −625.71 ($\omega_{1/2}$ 160 Hz).

2.3. Crystal Structure Determinations. Single crystals of (**1**)−(**4**) were grown from saturated acetonitrile solutions on prolonged standing at ambient temperature. Single-crystal X-ray diffraction intensities for compounds (**1**) and (**4**) were measured at 140 K on an Oxford Diffraction Xcalibur-3 CCD diffractometer, and for (**2**) and (**3**) at 120 K on a Bruker-Nonius Apex II Kappa-CCD diffractometer (at the EPSRC National Crystallography Service); both machines were equipped with Mo−Kα radiation and graphite monochromator. Intensity data were measured by thin-slice ω- and φ-scans.

The Xcalibur data were processed (including correcting for absorption) using the CrysAlis-CCD and -RED programs.[9] Crystal (**2**) was recognized as a nonmerohedral twin, and the Apex data for this crystal were processed with the EVAL program[10] with absorption corrections in TWINABS;[11] the Apex data for (**3**) were processed with the DENZO/SCALEPACK[12] programs and SADABS.[13] Structures were determined by the direct methods routines in the SHELXS program[14] and refined by full-matrix least-squares methods, on F^2's, in SHELXL.[14]

In (**1**), there is disorder in one of the *t*-butyl groups; one of the major component C atoms and the minor component C atoms were refined isotropically. There is an MeCN molecule in the cone of each calixarene ligand; these were fully resolved and their atoms were refined anisotropically. There are several more, partially occupied and not fully resolved MeCN molecules in the lattice; sixteen atom sites were identified, and these atoms were refined isotropically.

Disorder in three of the *t*-butyl groups of (**2**) was resolved except that one of the minor component methyl group C atoms was not located.

In compound (**3**), disorder in two *t*-butyl groups was identified and resolved clearly; alternative orientations in some other *t*-butyl groups have not been resolved. The limited data set allowed the refinement of only the V, O, and some N atoms with anisotropic thermal parameters; all remaining non-hydrogen atoms were refined isotropically.

All the remaining non-hydrogen atoms in (**1**) and (**2**), and all in (**4**) (where there was no disorder), were refined with anisotropic thermal parameters. Hydrogen atoms in the four complexes were included in idealized positions and their U_{iso} values were set to ride on the U_{eq} values of the parent carbon atoms.

Scattering factors for neutral atoms in all samples were taken from ref 15. Computer programs used in this analysis have been noted above, and were run through WinGX[16] on a Dell Precision 370 PC at the University of East Anglia. Crystal data and refinement results for the four complexes are collated in a table in the Supporting Information, together with the CIF files.

2.4. Polymerization of Ethylene. *Schlenk Line Procedure.* Ethylene polymerizations were carried out in flame-dried glass

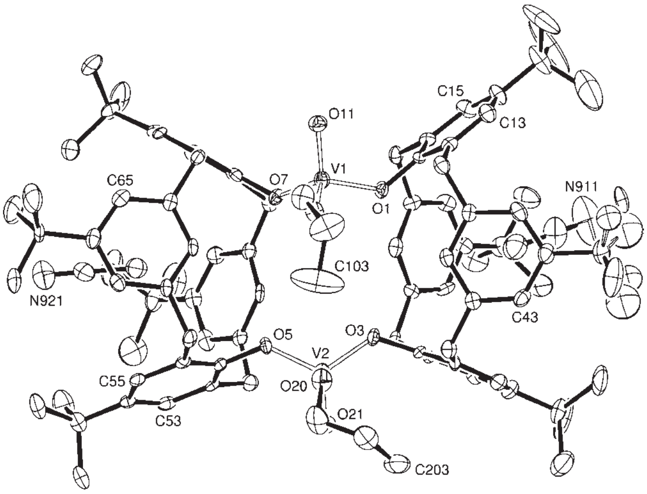

Figure 1. View of a molecule of $[VO(OnPr)L]_2$ (**1**) indicating the atom numbering scheme. Hydrogen atoms have been omitted for clarity. Thermal ellipsoids are drawn at the 50% probability level. Selected bond lengths (Å) and angles (deg): V(1)−O(1) 1.780(2), V(1)−O(7) 1.778(2), V(1)−O(10) 1.743(2), V(1)−O(11) 1.581(2), O(1)−V(1)−O(7) 111.93(10), O(1)−V(1)−O(10) 109.67(12), O(1)−V(1)−O(11) 106.97(12), O(10)−V(1)−O(7) 110.37(11), O(11)−V(1)−O(7) 110.17(12), O(11)−V(1)−O(10) 107.58(12).

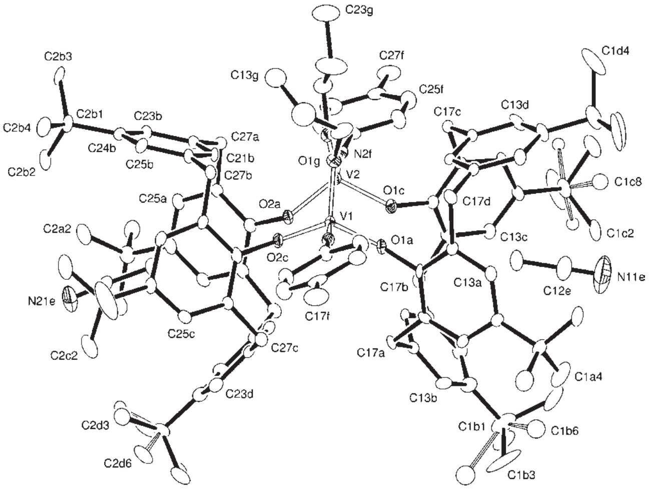

Figure 2. View of a molecule of $[V(Np\text{-tolyl})(OnPr)L]_2$ (**2**) indicating the atom numbering scheme. Hydrogen atoms have been omitted for clarity. Thermal ellipsoids are drawn at the 30% probability level. Selected bond lengths (Å) and angles (deg): V(1)−O(1A) 1.820(5), V(1)−O(2C) 1.792(6), V(1)−N(1F) 1.641(8), V(1)−O(1G) 1.790(6), N(1F)−V(1)−O(1A) 107.7(3), O(1G)−V(1)−O(1A) 111.8(3), O(2C)−V(1)−O(1A) 112.5(2), N(1F)−V(1)−O(1G) 103.6(3), N(1F)−V(1)−O(2C) 108.0(3), O(2C)−V(1)−O(1G) 112.7(3).

500 mL flasks with mechanical stirrer and temperature controller. The flask was evacuated and filled with ethylene gas at 1 bar pressure, which was maintained throughout the polymerization. Then predried and degassed toluene, the required amount of co-catalyst and reactivating agent (ETA) were added via glass syringe. The solution was stirred for approximately 10 min to allow ethylene saturation and the correct temperature to be acquired using a water bath. The pro-catalyst was injected as a toluene solution (prepared immediately prior to use). The polymerization was quenched by acidified methanol. The polymer was collected by filtration and dried overnight at 80 °C.

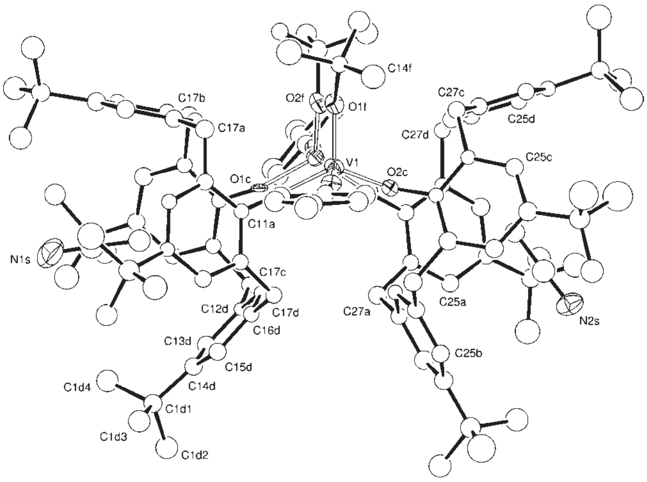

Figure 3. View of one of the three independent (but very similar) molecules of $[V(Np\text{-tolyl})(OtBu)L]_2$ (**3**), indicating the atom numbering scheme. Hydrogen atoms have been omitted for clarity. Thermal ellipsoids are drawn at the 30% probability level. Selected bond lengths (Å) and angles (deg): V(1)−O(1A) 1.829(12), V(1)−O(2C) 1.799(12), V(1)−N(1E) 1.649(14), V(1)−O(1F) 1.753(12), O(2C)−V(1)−O(1A) 112.7(4), N(1E)−V(1)−O(1A) 106.3(6), O(1F)−V(1)−O(1A) 114.0(5), N(1E)−V(1)−O(2C) 109.3(5), O(1F)−V(1)−O(2C) 109.2(4), N(1E)−V(1)−O(1F) 104.9(6).

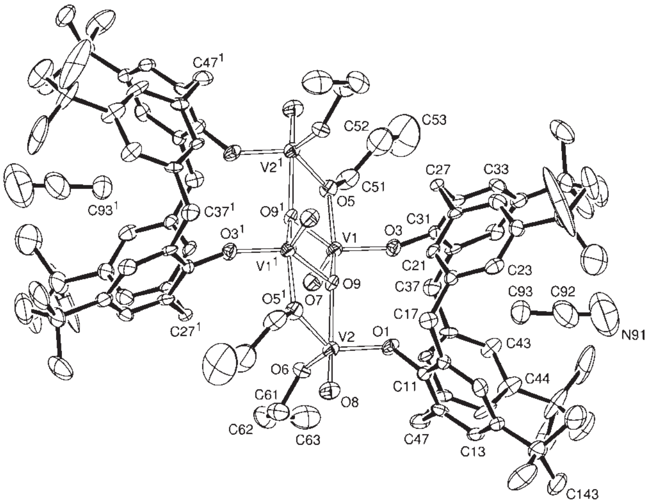

Figure 4. View of a molecule of $\{[VO(OnPr)]_2(\mu\text{-}O)L\}_2$ (**4**) indicating the atom numbering scheme. Hydrogen atoms have been omitted for clarity. Thermal ellipsoids are drawn at the 50% probability level. Selected bond lengths (Å) and angles (deg): V(1)−O(3) 1.766(4), V(1)−O(5) 2.042(4), V(1)−O(7) 1.573(4), V(1)−O(9) 1.857(4), V(1)−O(9^1) 1.877(4), O(3)−V(1)−O(5) 89.79(18), O(3)−V(1)−O(7) 109.0(2), O(3)−V(1)−O(9) 99.55(19), O(3)−V(1)−O(9^1) 137.16(17), V(1)−O(9)−V(2) 144.1(2), V(1)−O(9)−V(1^1) 100.4(2), O(8)−V(2)−O(9) 163.5(2).

Silica Supported Procedure. The procedure used the method referred to as pore-filling or incipient wetness to produce free-flowing powders that are easy to test.[17] The powders consist of a known quantity of pro-catalyst mixed with silica to produce the silica-catalyst. A 1 g portion of the supported catalyst was used in the test. The slurry polymerization

Table 1. Comparisons of Selected Dimensions of I (X = N-*p*-tolyl; R = *n*-Pr) and Complexes (1)−(4)

compound	I	1		2		3[a]		4	
V−O(2)[b], phenolate	1.836(2)	1.780(2)	1.790(2)	1.820(5)	1.793(5)	1.829(12)	1.802(12)	1.766(4)	1.795(4)
V−O(3), phenolate	1.856(2)	1.778(2)	1.785(2)	1.792(6)	1.815(5)	1.799(12)	1.808(11)		
V−N(1), N-*p*-tolyl	1.661(3)			1.641(8)	1.665(7)	1.649(14)	1.622(14)		
V−O, vanadyl		1.581(2)	1.575(2)					1.573(4)	1.578(4)
V−O(1), alkoxide	1.885(3)	1.743(2)	1.741(3)	1.790(6)	1.756(6)	1.753(12)	1.731(12)	2.042(4)	1.742(4)
V−O(1′), alkoxide	2.172(2)								1.906(4)
O/N(1)−V−O(1)	99.34(13)	107.58(12)	106.81(13)	103.6(3)	107.0(3)	104.9(6)	110.1(6)	99.9(2)	102.2(2)
O/N(1)−V−O(2)	99.11(13)	106.97(12)	109.67(13)	107.7(3)	104.7(3)	106.3(6)	107.3(6)	109.0(2)	99.1(2)
O/N(1)−V−O(3)	98.05(14)	110.17(12)	108.54(12)	108.0(3)	110.6(3)	109.3(5)	105.5(5)		
O/N(1)−V−O(1′)	170.74(13)								95.8(2)
O(2)−V−O(3)	110.39(12)	111.93(10)	111.91(12)	112.5(2)	113.6(3)	112.7(4)	113.8(4)		

[a] Dimensions are of one of the three independent molecules. [b] Atom names are those in compound **I**; the dimensions in complexes (**1**)−(**4**) are related by bond type.

tests using the silica-catalyst were carried out at 70 °C for 1 h, at 15.2 bar ethylene pressure, and using TiBAL [triisobutylaluminum] as a scavenger.

2.5. Polymerization of ε-Caprolactone. Schlenk tubes, equipped with magnetic stirrer bars, were dried in an oven at 170 °C for 12 h. and flame-dried under vacuum immediately before use. In a typical polymerization run, 20 mL of dry toluene was transferred into the Schlenk tube with the required amount of pro-catalyst. The solution was stirred and maintained at the desired temperature with the aid of an oil bath. Benzyl alcohol was then added from a 0.97 M solution in toluene. After approximately 5 min, the polymerization was started by the addition of the required equivalent of ε-caprolactone. At the end of the acquisition time, the polymerization was quenched by precipitating the polymer in methanol. After filtration, the polymer was left to dry in vacuo for 12 h.

3. RESULTS AND DISCUSSION

3.1. Synthesis and Characterization of Vanadium Complexes. Pro-ligand LH_2 was prepared following a previously reported procedure.[7] The vanadium systems were prepared by reacting 2.2 equiv of $[V(X)(OR)_3]$ (X = O, N*p*-tolyl; R = *n*Pr, *t*Bu) with 1 equiv of ligand in toluene and then refluxing the dark red solution for 12 h. Volatiles were then removed in vacuo, and the precipitate dissolved in hot acetonitrile. After cannula filtration, the red solution was then allowed to cool slowly to room temperature. Single crystals of (**1**)−(**4**) were formed after prolonged standing at room temperature. Their molecular structures were determined by X-ray diffraction methods; selected bond lengths, angles and the structures are given in Figures 1−4 for complexes (**1**)−(**4**), respectively, and are collated in Table 1. Use of only 1 equiv of vanadium precursor did not lead to increased yields, and such reactions often resulted in a dark brown oil.

In the dimeric structure of (**1**), one phenolic O atom from each calixarene ligand is linked through a VO(O*n*Pr) bridge; the second O atom from each calixarene ligand is bridged through a second VO(O*n*Pr) group. The two calixarene ligands (and the two bridging groups) are related by a pseudo-2-fold symmetry axis. Both vanadium centers are four-coordinate, with approximately tetrahedral geometries. There is an acetonitrile molecule in the cavities of both calixarene ligands.

The calixarene complex molecule of (**2**) and the three independent calixarene molecules in (**3**) are also dimer molecules, and resemble (**1**) in many respects. Each comprises two vanadium atoms (four-coordinate, with tetrahedral coordination pattern) linked through the phenolate O atoms of the two calixarene ions. There are also O*n*Pr (or O*t*Bu) and N*p*-tolyl ligands on each vanadium atom, and an acetonitrile molecule lies in the cone of each calixarene unit. The whole molecule is arranged with approximately 2*mm* symmetry. The pseudo-2-fold axis passes through the midpoint of the V···V vector and relates the pairs of O*n*Pr (or O*t*Bu), N*p*-tolyl and calixarene ligands.

Complex (**4**) (Figure 4) was formed as a minor side product through the partial hydrolysis of complex (**1**) during the reaction. The incorporation of 2 equiv of water has led to the formation of a vanadium−oxygen cage between the two depleted calix[4]arene ligands.

The complex dimeric molecule (**4**) lies about a center of symmetry. The two calixarene ligands are linked through a V_4O_4 network. Each vanadium atom is 5-coordinate: V(1) has a square pyramidal pattern with the vanadyl oxygen, O(7), in the apical site, whereas the pattern of V(2) is closer to trigonal bipyramidal with the vanadyl O(8) and a μ^3-O atom, O(9), in the axial positions. Both metals are bonded to a vanadyl O, a phenolic O, and a bridging O*n*Pr ligand; the shell of V(1) is completed by two μ^3-O ligands, whereas V(2) has one μ^3-O and a terminal O*n*Pr ligand. There is a molecule of solvent, acetonitrile, in the cone cavity of each calixarene ligand.

The depleted calixarenes in (**1**)−(**4**) can be viewed as diphenolate ligands, and as such can be compared with recently reported vanadium-based diphenolate pro-catalysts such as the imido alkoxide **I** (Chart 2)[18] Inspection of selected geometrical parameters (see Table 1) associated with (**1**)−(**4**) and **I** reveals that many of the bond lengths and angles in such systems are very similar. However, differences arise because of the 1,3-disposition of the phenolate oxygen atoms on the depleted calixarenes compared with those in the diphenolate ligands of **I** (X = N-*p*-tolyl, R = *i*Pr), the latter forming an eight-membered metallocyclic ring adopting a flattened chair conformation. We also note that a number of 1,3-dimethylether-p-*tert*-butylcalix[4]areneH_2 derived vanadium complexes of type **II** have been structurally characterized, in which two vanadium atoms are bound to the one calix[4]arene ligand (similar to each depleted calix[4]arene in **4**).[2] Complexes of types **I** and **II**, together with other related vanadium-containing calix[4]arene species (see Chart 2), will be discussed in the polymerization sections below.

3.2. Polymerization of Ethylene. Complexes (**1**)−(**4**) have been evaluated as pro-catalysts for the polymerization

Chart 2. Related Vanadium-Based Pro-Catalyst II–VI (R = *tert*-butyl)

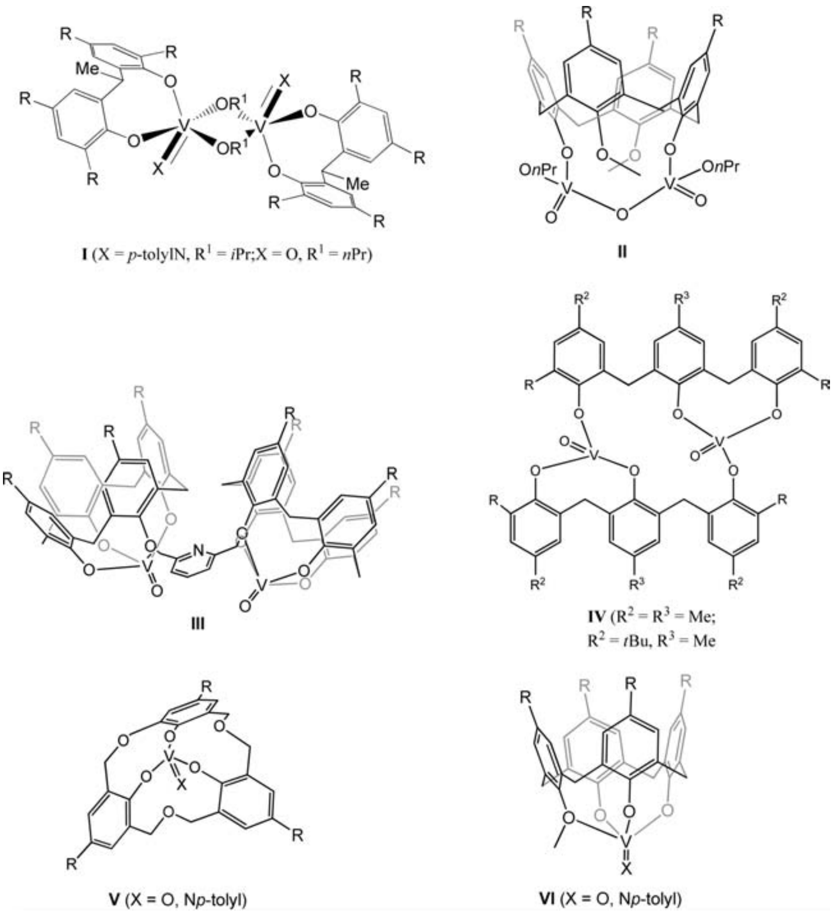

I (X = *p*-tolylN, R^1 = *i*Pr;X = O, R^1 = *n*Pr)

II

III

IV (R^2 = R^3 = Me; R^2 = *t*Bu, R^3 = Me

V (X = O, N*p*-tolyl)

VI (X = O, N*p*-tolyl)

of ethylene, employing either DMAC (dimethylaluminum chloride) or MADC (methylaluminum dichloride) as co-catalyst, with ETA (ethyltrichloroacetate) present. Polymerizations were carried out in toluene (200 mL) using 1000–8000 molar equiv of co-catalyst over a range of temperatures (20–80 °C) over 15 min unless otherwise stated. Representative results are presented in Tables 2 and 3.

Pro-catalysts (**1**) and (**2**) behave similarly when using either DMAC or MADC as co-catalyst. In particular, both exhibit enhanced catalytic activity (runs 3 and 20–DMAC; runs 11 and 28–MADC) at elevated temperature (80 °C). Furthermore, a gradual increase in observed activity occurs on increasing co-catalyst concentration, though in the case of (**2**), the activity peaks at 6000 equiv for MADC (run 33). For the *tert*-butoxide (**3**), the thermal stability is reduced, such that highest activities were observed at 40 °C (run 36) when using DMAC, and 60 °C (run 45) when using MADC. In each case though, the previous trend of increased activity on increasing cocatalyst concentration was observed. For pro-catalyst (**4**), enhanced thermal stability was observed at 80 °C in the presence of both DMAC (run 56) and MADC (run 59). At 80 °C, in the presence of 2000 equiv of cocatalyst, the activity orders (**4**) ≈ (**1**) > (**2**) > (**3**) for DMAC and (**4**) > (**1**) ≈ (**2**) > (**3**) for MADC were observed. In general, there was a change in the polymer morphology (from a thick jelly like solid to a fine white powder) at higher temperatures, which started at about 60 °C. Pro-catalyst (**1**) was also screened under more industrially relevant conditions using either TEA [triethylaluminum] (1.5×10^{-4} moles, 11 equiv) or DEAC [diethylaluminum chloride] as cocatalyst (1.5×10^{-4} moles, 15 equiv). At 220 °C and 29 bar, ethylene fed in on demand, and in the presence of hydrogen, a 10 min run did not yield any polymeric products.[17] Both (**1**) and (**2**) were also supported on silica and screened under slurry conditions (see Table 3). In this case, polymer was formed, but activities were ≤30 g/mmol hr.

Comparison of the homogeneous results obtained using (**1**)–(**4**) with those previously reported for the systems **I**–**VII** (Table 4), shows that the results herein are more akin to those observed for other multimetallic calix[4]arene species such as **II** and **III**. Activities, particularly at elevated temperatures, associated with di- and triphenolates (**I** and **IV**) and oxacalix-[3]arene-based complexes (**V**) were far superior, whereas those observed for monomeric methylether-p-*tert*-butylcalix-[4]arene complexes (**VI**) and for dimeric structures of the type [Vcalix[4]arene(O) $_4$(NCMe)]$_2$ (**VII**), were almost an order of magnitude lower.[2]

3.3. Polymerization of ε-Caprolactone. Complexes (**1**)–(**3**) were also screened for their ability to polymerize ε-caprolactone at 80 °C (no polymer formed at room temperature, and little below 80 °C). The polymerization data are presented in Table 5.

The vanadyl complex showed good conversion (94%), whereas the imido complexes (**2**) and (**3**) exhibited far poorer

Table 2. Results for Ethylene Polymerization Runs (Schlenk Conditions) Using Pro-Catalysts (1)−(4)[a]

run	pro-catalyst (μmol)	co-catalyst	[Al]/[V]	time (min)	temp (°C)	yield PE/g[c]	activity[d]
1	**1** (0.25)	DMAC	2000	15	20	1.34	5.36
2	**1** (0.25)	DMAC	2000	15	40	2.07	8.28
3	**1** (0.25)	DMAC	2000	15	80	3.95	15.8
4	**1** (0.25)	DMAC	2000	15	20	1.52	6.08
5	**1** (0.25)	DMAC	4000	15	20	2.04	8.16
6[b]	**1** (0.15)	DMAC	6000	10	20	1.55	10.3
7[b]	**1** (0.15)	DMAC	8000	10	20	2.19	14.6
8	**1** (0.25)	MADC	2000	15	20	1.96	7.84
9	**1** (0.25)	MADC	2000	15	40	2.78	11.1
10	**1** (0.25)	MADC	2000	15	60	2.18	8.72
11	**1** (0.25)	MADC	2000	15	80	2.63	10.5
12	**1** (0.25)	MADC	1000	15	20	1.48	5.92
13	**1** (0.25)	MADC	2000	15	20	1.49	5.96
14	**1** (0.25)	MADC	4000	15	20	1.90	7.60
15[b]	**1** (0.15)	MADC	6000	10	20	1.79	11.9
16[b]	**1** (0.15)	MADC	8000	10	20	1.95	13.0
17	**2** (0.25)	DMAC	2000	15	20	1.08	4.32
18	**2** (0.25)	DMAC	2000	15	40	1.56	6.24
19	**2** (0.25)	DMAC	2000	15	60	1.86	7.56
20	**2** (0.25)	DMAC	2000	15	80	2.65	10.6
21	**2** (0.25)	DMAC	1000	15	20	1.25	5.00
22	**2** (0.25)	DMAC	3000	15	20	1.37	5.48
23[b]	**2** (0.15)	DMAC	6000	10	20	1.41	9.40
24[b]	**2** (0.15)	DMAC	8000	10	20	1.99	13.3
25	**2** (0.25)	MADC	2000	15	20	1.12	4.48
26	**2** (0.25)	MADC	2000	15	40	1.59	6.36
27	**2** (0.25)	MADC	2000	15	60	1.60	6.40
28	**2** (0.25)	MADC	2000	15	80	2.51	10.0
29	**2** (0.25)	MADC	1000	15	20	0.60	2.40
30	**2** (0.25)	MADC	2000	15	20	1.38	5.52
31	**2** (0.25)	MADC	3000	15	20	1.99	7.96
32	**2** (0.25)	MADC	4000	15	20	2.51	10.0
33[b]	**2** (0.15)	MADC	6000	10	20	2.07	13.8
34[b]	**2** (0.15)	MADC	8000	10	20	1.85	12.3
35	**3** (0.25)	DMAC	2000	15	20	1.65	6.60
36	**3** (0.25)	DMAC	2000	15	40	2.55	10.2
37	**3** (0.25)	DMAC	2000	15	60	1.33	5.32
38	**3** (0.25)	DMAC	2000	15	80	1.11	4.44
39	**3** (0.25)	DMAC	1000	15	20	1.95	7.80
40	**3** (0.25)	DMAC	3000	15	20	2.06	8.24
41[b]	**3** (0.15)	DMAC	6000	10	20	1.03	6.87
42[b]	**3** (0.15)	DMAC	8000	10	20	1.42	9.47
43	**3** (0.25)	MADC	2000	15	20	1.44	5.76
44	**3** (0.25)	MADC	2000	15	40	1.48	5.92
45	**3** (0.25)	MADC	2000	15	60	2.08	8.32
46	**3** (0.25)	MADC	2000	15	80	0.95	3.80
47	**3** (0.25)	MADC	1000	15	20	1.23	4.92
48	**3** (0.25)	MADC	2000	15	20	1.40	5.60
49	**3** (0.25)	MADC	3000	15	20	1.76	7.04
50	**3** (0.25)	MADC	4000	15	20	2.72	10.9
51[b]	**3** (0.15)	MADC	6000	10	20	1.16	7.73
52[b]	**3** (0.15)	MADC	8000	10	20	2.00	13.3
53	**4** (0.25)	DMAC	2000	15	20	2.47	9.88
54	**4** (0.25)	DMAC	2000	15	40	2.49	9.96

Table 2. Continued

run	pro-catalyst (μmol)	co-catalyst	[Al]/[V]	time (min)	temp (°C)	yield PE/g[c]	activity[d]
55	**4** (0.25)	DMAC	2000	15	60	3.27	13.1
56	**4** (0.25)	DMAC	2000	15	80	4.10	16.4
57	**4** (0.25)	MADC	2000	15	20	1.26	5.04
58	**4** (0.25)	MADC	2000	15	40	1.99	7.96
59	**4** (0.25)	MADC	2000	15	80	2.99	12.0

[a] 1 bar ethylene Schlenk tests carried out in toluene (200 mL) in the presence of ETA (0.05 mL) over 15 min; reaction was quenched with dilute HCl, washed with methanol (50 mL) and dried for 12 h. at 80 °C. [b] 0.025 mL of ETA. [c] g per pro-catalyst. [d] g/mmol h bar ($\times 10^3$).

Table 3. Results for Ethylene Polymerization Runs (Supported Silica-Catalyst) Using Pro-Catalysts (1) and (2)[a]

run	pro-catalyst (μmol)	co-catalyst	[Al]/[V]	time (min)	temp (°C)	yield PE/g	activity[b]
1	**1** (5.0)	MAO	1700	60	70	4.02	30
2	**2** (5.1)	MAO	1650	60	70	1.80	10
3	**2** (3.0)	DEAC	1600	60	70	0.60	10

[a] 15.2 bar ethylene partial pressure slurry polymerization tests carried out in isobutane in the presence of TiBAL as scavenger. [b] g mmol h bar per V center.

Table 4. Ethylene Polymerization Behavior of Pro-Catalysts I–VII

pro-catalyst	activity (g/mmol h bar)	*T* (°C)	Al/V ratio	time (min)
I (X = O)	37,400	25	2,500	15
	157,000	80	2,500	15
I (X = N-*p*-tolyl)	38,800	45	40,000	30
II	8,700	45	4,000	60
III	10,400	45	10,000	60
IV	46,100	25	2,500	15
	156,000	80	2,500	15
V (X = O)	25,300	25	2,500	15
	92,500	80	2,500	15
V (X = N-*p*-tolyl)	13,400	25	2,500	15
	129,400	80	2,500	15
VI (X = O)	1,400	45	4,000	60
VI (X = N-*p*-tolyl)	1,500	45	4,000	60
VII	1,300	45	4,000	60

Table 5. ε-Caprolactone Screening Results for Complexes (1)–(3)[a]

run	pro-catalyst	conversion[b] (%)	M_n calculated[c] (g/mol)	M_n measured[d] (g/mol)	PDI
1	**1**	94	45,7	3.1	1.1
2	**2**	46	12.3	3.9	1.1
3	**3**	20	23.7	5.4	1.3

[a] Conditions: monomer/metal = 400; 72 h; 80 °C; 20 mL of toluene; 2 mL of ε-caprolactone; 5 equiv of benzyl alcohol (from a 0.97 M solution in toluene). [b] Calculated by ^{1}H NMR. [c] $\times 10^3$. [d] Mn measured = 0.58 × Mn GPC $\times 10^3$.[19]

conversions. Given that (**2**) and (**3**) are essentially isostructural, we can infer here that the presence of the bulkier alkoxide (*t*Bu) in (**3**) is the reason for the poorer conversion compared with (**2**) (*n*Pr). Only low molecular weight polymers were obtained. All polymers were of low polydispersity (≤1.3), which suggested that these polymerizations occurred without side reactions. For comparison, results obtained when using complex **I** were ∼60% conversion after 24 h at 60 °C, affording a polymer with molecular weight of about 11,000 with PDI ∼1.1.[18]

4. CONCLUSION

We have isolated and characterized new dimeric oxo and imido vanadium complexes of the form $[VX(OR)L]_2$ bearing 1,3-depleted calix[4]arene ligands L. Under Schlenk conditions, using DMAC as co-catalyst (1000 to 8000 equiv) and in the presence of the reactivator ETA, such complexes are highly active (≤16,400 g/mmol h bar) for the polymerization of ethylene over the temperature range 20 to 80 °C. Under slurry conditions using a silica support, activities for (**1**) and (**2**) were somewhat disappointing (≤30 g/mmol h), and this was thought to be due to problems associated with supporting these pro-catalysts. For ε-caprolactone polymerization, vanadyl complex (**1**) exhibited high conversion (94%), whereas the imido species were less efficient with conversions of 46% (**2**) and 20% (**3**).

■ ASSOCIATED CONTENT

Ⓢ Supporting Information. X-ray crystallographic data for the structure determinations of compounds (**1**)–(**4**), together with the CIF files for the four structures. This material is available free of charge via the Internet at http://pubs.acs.org.

■ AUTHOR INFORMATION

Corresponding Author

*E-mail: carl.redshaw@uea.ac.uk.

■ ACKNOWLEDGMENT

The EPSRC is thanked for financial support. The EPSRC Mass Spectrometry Service (Swansea, U.K.) and the EPSRC National Crystallography Service (Southampton) are thanked for data. We also thank Dr. Sandor Nagy, Dr. Mark Reinking, and Karen Neal-Hawkins (Equistar Chemicals) for help with high pressures and slurry polymerization measurements.

REFERENCES

(1) Redshaw, C.; Homden, D. M. *Chem. Rev.* **2008**, *108*, 5086.

(2) Redshaw, C.; Rowan, M. A.; Warford, L.; Homden, D. M.; Arbaoui, A.; Elsegood, M. R. J.; Dale, S. H.; Yamato, T.; Casas, C. P.; Matsui, S. *Chem.—Eur. J.* **2007**, *13*, 1090.

(3) Redshaw, C.; Warford, L.; Dale, S. H.; Elsegood, M. R. J. *Chem. Commun.* **2004**, 1954.

(4) Grynszpan, F.; Goren, Z.; Biali, S. E. *J. Org. Chem.* **1991**, *56*, 532.

(5) Tzadka, E.; Goldberg, I.; Vigalok, A. *Chem. Commun.* **2009**, 2041.

(6) Nagy, S. United States Patent No. US 6,984,599 B2, Jan 10, 2006.

(7) (a) Espinas, J.; Darbost, U.; Pelletier, J.; Jeanneau, E.; Duchamp, C.; Bayard, F.; Boyron, O.; Thivolle-Cazart, J.; Basset, J.-M.; Taoufik., M.; Bonnamour, I. *Eur. J. Inorg. Chem.* **2010**, *9*, 1349.(b) Espinas, J.; Pelletier, J.; Jeanneau, E.; Darbost, U.; Szeto, K. C.; Lucas, C.; Thivolle-Cazart, J.; Duchamp, C.; Henriques, N.; Bouchu, D.; Basset, J.-M.; Chermette, H.; Bonnamour, I.; Taoufik. M. *Organometallics*, **2011**, advanced article DOI: 10.1021/om200140u.

(8) Lutz, M.; Hagen, H.; Antoine, S. M. M.; Soek, A. L.; van Koten, G. *Acta Crystallogr.* **1999**, *55*, 1636.

(9) *CrysAlisPro*; Oxford Diffraction Ltd.: Abingdon, U.K., 2010.

(10) Duisenberg, A. J. M.; Kroon-Batenburg, L. M. J.; Schreurs, A. M. M. *VAL-14, An intensity evaluation method*; *J. Appl. Crystallogr.* 2003, 36, 220.

(11) Sheldrick, G. M. *TWINABS, Program for calculation of absorption corrections for area-detector systems*, Version 2007/2; Bruker AXS Inc.: Madison, WI, 2007.

(12) Otwinowski, Z.; Minor, W. Processing of X-ray diffraction data collected in oscillation mode. In *Methods in Enzymology*; Carter, C. W., Jr., Sweet, R. M., Eds.; Academic Press: New York, 1997; Vol. 276, Macromolecular Crystallography, Part A, pp 307−326.

(13) Sheldrick, G. M. *SADABS, Program for calculation of absorption corrections for area-detector systems*, Version 2007/2. Bruker AXS Inc.: Madison, WI, 2007.

(14) Sheldrick, G. M. *SHELX-97, Programs for crystal structure determination (SHELXS) and refinement (SHELXL)*; *Acta Crystallogr.* 2008, A64, 112.

(15) *International Tables for X-ray Crystallography*; Kluwer Academic Publishers: Dordrecht, The Netherlands, 1992; Vol. C, pp 500, 219, and 193.

(16) Farrugia, L. J. *J. Appl. Crystallogr.* **1999**, *32*, 837.

(17) Arbaoui, A.; Redshaw, C.; Homden, D. M.; Wright, J. A.; Elsegood, M. R. J. *Dalton Trans.* **2009**, 8911.

(18) Nagy S. (Equistar Chemicals), Personal Communication.

(19) Kowalski, A.; Duda, A.; Penczek, S. *Macromolecules* **1998**, *31*, 2114.